

Warped flavor symmetry predictions for neutrino physics

Peng Chen,^{1,*} Gui-Jun Ding,^{1,†} Alma. D. Rojas,^{2,‡} C. A. Vaquera-Araujo,^{2,§} and J. W. F. Valle^{2,¶}

¹*Department of Modern Physics, University of Science and Technology of China
Hefei, Anhui 230026, CHINA*

²*AHEP Group, Institut de Física Corpuscular – C.S.I.C./Universitat de València, Parc Científic de Paterna.
C/Catedrático José Beltrán, 2 E-46980 Paterna (València) - SPAIN*

A realistic five-dimensional warped scenario with all standard model fields propagating in the bulk is proposed. Mass hierarchies would in principle be accounted for by judicious choices of the bulk mass parameters, while fermion mixing angles are restricted by a $\Delta(27)$ flavor symmetry broken on the branes by flavon fields. The latter gives stringent predictions for the neutrino mixing parameters, and the Dirac CP violation phase, all described in terms of only two independent parameters at leading order. The scheme also gives an adequate CKM fit and should be testable within upcoming oscillation experiments.

PACS numbers: 14.60.Pq, 11.30.Er

I. INTRODUCTION

The understanding of flavor constitutes one of the most stubborn open challenges in particle physics [1]. Two aspects of the problem are the understanding of fermion mass hierarchies as well as mixing parameters. Various types of flavor symmetries have been invoked in this context [2–9]. These efforts have been partly motivated by the original success of the tri-bimaximal mixing ansatz [10]. The resulting non-Abelian flavor symmetries are typically broken spontaneously down to two different residual subgroups in the neutrino and the charged lepton sectors, leading to zero reactor mixing parameter, $\theta_{13} = 0$. However, the measurement of a non-zero value for the reactor angle [11–14] implies the need to revamp the original flavor symmetry-based approaches in order to generate $\theta_{13} \neq 0$ [15] or else look for alternative possibilities, such as bi-large neutrino mixing [16–18].

The existence of warped extra-dimensions has been advocated by Randall & Sundrum [19] as a way to address the hierarchy problem, since the fundamental scale of gravity is exponentially reduced from the Planck mass down to the TeV scale as a result of having the Higgs sector localized near the boundary of the extra dimensions. Moreover, if standard model fermions are allowed to propagate in the bulk and also become localized towards either brane, the scenario can also address the flavor problem possibly acting in synergy with the flavor group predictions. This is what we do in the present paper.

The idea of combining discrete flavor symmetries and extra dimensions is quite attractive and has already been discussed in the literature within the context of large extra dimensions [20–22], warped extra dimensions [23–27] and holographic composite Higgs models [28–30]. However, such models try to generate tri-bimaximal neutrino mixing, which has been ruled out by the measurement of the reactor angle θ_{13} [11–14] and also global fits of neutrino oscillation data [31]. One of us has constructed a warped extra dimension model with S_4 flavor symmetry where democratic mixing is produced at leading order and non-zero θ_{13} can arise from subleading corrections [32]. In this work, we shall re-consider the issue of predicting flavor properties in particle physics by combining the conventional predictive power

*Electronic address: pche@mail.ustc.edu.cn

†Electronic address: dinggj@ustc.edu.cn

‡Electronic address: alma.rojas@ific.uv.es

§Electronic address: vaquera@ific.uv.es

¶Electronic address: valle@ific.uv.es; URL:<http://astroparticles.es/>

inherent in the use of non-Abelian flavor symmetries with the presence of warped extra-dimensions. We propose a warped five-dimensional scenario in which all matter fields propagate in the bulk and neutrinos are treated as Dirac particles. Our model can accommodate all the strengths of the standard model Yukawa couplings and resulting fermion mass hierarchies by making adequate choices of fermion bulk mass parameters, while the fermion mixing parameters can be restricted by means of the assumed flavor symmetry. We present a $\Delta(27)$ based flavor symmetry which nicely describes the neutrino oscillation parameters in terms of just two independent parameters, leading to interesting correlations involving the neutrino mass hierarchy and the leptonic Dirac CP phase, not yet reliably determined by current global oscillation fit [31]. Our predictions include a neat leading order relation between the solar and reactor mixing parameters which should be tested at future oscillation experiments.

II. BASIC STRUCTURE OF THE MODEL

In this section we present the basic setup of a warped five-dimensional (5D) model for fermions, constructed under a $\Delta(27) \otimes Z_4 \otimes Z'_4$ flavor symmetry. The 5D field theory is defined on a slice of AdS_5 , where the bulk geometry is described by the metric

$$ds^2 = e^{-2ky} \eta_{\mu\nu} dx^\mu dx^\nu - dy^2, \quad (1)$$

with $\eta_{\mu\nu} = \text{diag}(1, -1, -1, -1)$ and k as the AdS_5 curvature scale. The fifth dimension y is compactified on S_1/Z_2 , and two flat 3-branes of opposite tension are attached to the orbifold fixed points, located at $y = 0$ (UV brane) and $y = L$ (IR brane).

The electroweak symmetry of the model is promoted to $G_{\text{bulk}} = SU(2)_L \otimes SU(2)_R \otimes U(1)_{B-L}$ in order to avoid excessive contributions to the Peskin-Takeuchi T parameter [33, 34]. The gauge group G_{bulk} breaks down to the standard model electroweak (EW) group $G_{\text{SM}} = SU(2)_L \otimes U(1)_Y$ on the UV brane by the boundary conditions (BCs) of the gauge bosons. Furthermore, a bulk Higgs field with $(SU(2)_L, SU(2)_R)$ quantum numbers

$$H \sim (\mathbf{2}, \mathbf{2}) \quad (2)$$

is responsible for the spontaneous symmetry breaking (SSB) of G_{SM} . The 5D Higgs field $H(x^\mu, y)$ can be decomposed into Kaluza-Klein (KK) modes as

$$H(x^\mu, y) = H(x^\mu) \frac{f_H(y)}{\sqrt{L}} + \text{heavy KK Modes}. \quad (3)$$

For an adequate choice of BCs, its zero mode profile $f_H(y)$ can be written as [35]

$$f_H(y) = \sqrt{\frac{2kL(1-\beta)}{1-e^{-2(1-\beta)kL}}} e^{kL} e^{(2-\beta)k(y-L)}, \quad (4)$$

where we have introduced the Higgs localization parameter $\beta = \sqrt{4 + m_H^2/k^2}$ in terms of the Higgs field bulk mass parameter m_H . In the present work, we assume that the vacuum expectation value (VEV) of the Higgs zero mode is of the form

$$\langle H(x^\mu) \rangle = \frac{v_H}{\sqrt{2}} \begin{pmatrix} 1 & 0 \\ 0 & 1 \end{pmatrix}, \quad (5)$$

and it is peaked toward the IR brane, allowing for a TeV scale EW SSB and inducing the G_{bulk} breakdown to $SU(2)_D \otimes U(1)_{B-L}$ on that brane.

Three families of fermion fields are required to describe each generation (labeled by $i = 1, 2, 3$) of quarks and leptons. All fermion fields propagate into the bulk and transform under the minimal representation of the gauge

group $SU(2)_L \otimes SU(2)_R$ [33, 34]. In the lepton sector the three multiplets of the model are given as

$$\Psi_{\ell_i} = \begin{pmatrix} \nu_i^{[++]} \\ e_i^{[++]} \end{pmatrix} \sim (\mathbf{2}, \mathbf{1}), \quad \Psi_{e_i} = \begin{pmatrix} \nu_i^{[+-]} \\ e_i^{[-]} \end{pmatrix} \sim (\mathbf{1}, \mathbf{2}), \quad \Psi_{\nu_i} = \begin{pmatrix} \nu_i^{[-]} \\ e_i^{[+-]} \end{pmatrix} \sim (\mathbf{1}, \mathbf{2}), \quad (6)$$

while for the quark sector we have

$$\Psi_{Q_i} = \begin{pmatrix} u_i^{[++]} \\ d_i^{[++]} \end{pmatrix} \sim (\mathbf{2}, \mathbf{1}), \quad \Psi_{d_i} = \begin{pmatrix} u_i^{[+-]} \\ d_i^{[-]} \end{pmatrix} \sim (\mathbf{1}, \mathbf{2}), \quad \Psi_{u_i} = \begin{pmatrix} u_i^{[-]} \\ d_i^{[+-]} \end{pmatrix} \sim (\mathbf{1}, \mathbf{2}). \quad (7)$$

Notice that we have a separate $SU(2)_R$ doublet for every right handed fermion. In the above equations, fields with different sign assignments must be understood as independent. The bracketed signs indicate Neumann (+) or Dirichlet (−) BCs for the left-handed component of the corresponding field, on both UV and IR branes. The right-handed part of the field satisfies opposite BCs. Only fields with $[++]$ BCs have left-handed zero modes, whereas right-handed zero modes exist solely for fields with $[-]$ BCs. The KK decomposition for such fields has the form

$$\begin{aligned} \psi^{[++]}(x^\mu, y) &= \frac{e^{2ky}}{\sqrt{L}} \left\{ \psi_L(x^\mu) f_L^{(0)}(y, c_L) + \text{heavy KK modes} \right\}, \\ \psi^{[-]}(x^\mu, y) &= \frac{e^{2ky}}{\sqrt{L}} \left\{ \psi_R(x^\mu) f_R^{(0)}(y, c_R) + \text{heavy KK modes} \right\}, \end{aligned} \quad (8)$$

with $\psi = \nu_i, e_i, u_i, d_i$, and zero mode profiles [36–38]

$$f_L^{(0)}(y, c_L) = \sqrt{\frac{(1-2c_L)kL}{e^{(1-2c_L)kL} - 1}} e^{-c_L ky}, \quad f_R^{(0)}(y, c_R) = \sqrt{\frac{(1+2c_R)kL}{e^{(1+2c_R)kL} - 1}} e^{c_R ky}, \quad (9)$$

where c_L and c_R are the bulk mass parameters of the 5D fermion fields in units of the AdS_5 curvature k . Thus, the low energy spectrum contains left-handed doublets $\ell_{iL} = (\nu_{iL}, e_{iL})$, $Q_{iL} = (u_{iL}, d_{iL})$, alongside right-handed singlets $\nu_{iR}, e_{iR}, u_{iR}, d_{iR}$. In the following, we identify all standard model fields with this set of zero modes (*i.e.* the so called zero mode approximation, ZMA). For future convenience, we denote the flavor components of charged leptons and quarks as $e_{1,2,3} = e, \mu, \tau$; $Q_{1,2,3} = U, C, T$; $u_{1,2,3} = u, c, t$; $d_{1,2,3} = d, s, b$.

In the present work, we choose the flavor symmetry to be $\Delta(27)$, augmented by the auxiliary symmetry $Z_4 \otimes Z'_4$. The group $\Delta(27)$ was originally proposed to explain the fermion masses and flavor mixing in Refs. [39, 40], and has been used for Dirac neutrinos in [41] by one of us. Here we study its implementation in a warped extra dimensional theory. The flavor symmetry $\Delta(27) \otimes Z_4 \otimes Z'_4$ is broken by brane localized flavons, transforming as singlets under G_{bulk} . We introduce a set of flavons ξ, σ_1, σ_2 localized on the IR brane, and a flavon φ localized on the UV brane. Both ξ and φ are assigned to the three dimensional representation $\mathbf{3}$ of $\Delta(27)$, while σ_1 and σ_2 transform as inequivalent one dimensional representations $\mathbf{1}_{0,1}$ and $\mathbf{1}_{0,0}$ respectively. A summary of the $\Delta(27)$ group properties and its representations can be found in Appendix A. There are two different scenarios for the model, determined by the two possible VEV alignments for ξ , namely:

$$\begin{aligned} \langle \xi \rangle &= (0, 1, 0) v_\xi, & \text{Case I,} \\ \langle \xi \rangle &= (1, \omega, 1) v_\xi, & \text{Case II,} \end{aligned} \quad (10)$$

with $\omega = e^{2\pi i/3}$. As indicated above, we will denote the models described by each alignment as cases I and II, respectively. Note that the case II vacuum pattern frequently appears in the context of geometrical CP violation [42, 43]. The VEVs for the remaining flavon fields are

$$\langle \varphi \rangle = (1, 1, 1) v_\varphi, \quad \langle \sigma_1 \rangle = v_{\sigma_1}, \quad \langle \sigma_2 \rangle = v_{\sigma_2}. \quad (11)$$

Further details regarding this vacuum configuration are offered in Appendix B.

III. LEPTON SECTOR

Once the basic framework has been laid out, we are in position to discuss the structure of the lepton sector and its phenomenological implications. As we will show below, charged lepton as well as Dirac neutrino masses are generated at leading order (LO), and non-zero values for the ‘‘reactor angle’’ θ_{13} arise naturally. The model is predictive, in the sense that the three mixing angles and the Dirac CP phase will ultimately be determined in terms of only two parameters.

A. Lepton masses and mixing

Field	Ψ_ℓ	Ψ_e	Ψ_μ	Ψ_τ	Ψ_{ν_1}	Ψ_{ν_2}	Ψ_{ν_3}	H	φ	ξ	σ_1	σ_2
$\Delta(27)$	3	$\mathbf{1}_{0,0}$	$\mathbf{1}_{1,0}$	$\mathbf{1}_{2,0}$	$\mathbf{1}_{0,0}$	$\mathbf{1}_{0,0}$	$\mathbf{1}_{0,0}$	$\mathbf{1}_{0,0}$	3	3	$\mathbf{1}_{0,1}$	$\mathbf{1}_{0,0}$
Z_4	1	1	1	1	-1	i	-1	1	1	-1	1	i
Z'_4	1	i	i	i	-1	-1	-1	1	$-i$	1	-1	-1

TABLE I: Particle content and transformation properties of the lepton and scalar sectors under the flavor symmetry $\Delta(27) \otimes Z_4 \otimes Z'_4$.

The transformation properties of leptons and scalars under the family symmetry $\Delta(27) \otimes Z_4 \otimes Z'_4$ are given in Table I. Note that the Higgs field is inert under the flavor symmetry. Since the three left-handed lepton doublets are unified into a faithful triplet **3** of $\Delta(27)$, they will share one common bulk mass parameter c_ℓ . On the other hand, both right-handed charged leptons and right-handed neutrinos are assigned to singlet representations of $\Delta(27)$. Therefore, there are six different bulk mass parameters c_{e_i} and c_{ν_i} ($i = 1, 2, 3$) for these fields. From the particle transformation properties we can write the most general lepton Yukawa interactions that are both gauge and flavor invariant at LO:

$$\begin{aligned}
\mathcal{L}_Y^l = & \frac{\sqrt{G}}{\Lambda^{\frac{5}{2}}} \left\{ y_e (\varphi \bar{\Psi}_\ell)_{\mathbf{1}_{0,0}} H \Psi_e + y_\mu (\varphi \bar{\Psi}_\ell)_{\mathbf{1}_{2,0}} H \Psi_\mu + y_\tau (\varphi \bar{\Psi}_\ell)_{\mathbf{1}_{1,0}} H \Psi_\tau \right\} \delta(y) \\
& + \frac{\sqrt{G}}{(\Lambda')^{\frac{7}{2}}} \left\{ y_{11} (\xi \sigma_1 \bar{\Psi}_\ell)_{\mathbf{1}_{0,0}} \tilde{H} \Psi_{\nu_1} + y_{31} (\xi \sigma_1^* \bar{\Psi}_\ell)_{\mathbf{1}_{0,0}} \tilde{H} \Psi_{\nu_1} + y_{22} (\xi \sigma_2 \bar{\Psi}_\ell)_{\mathbf{1}_{0,0}} \tilde{H} \Psi_{\nu_2} \right. \\
& \left. + y_{13} (\xi \sigma_1 \bar{\Psi}_\ell)_{\mathbf{1}_{0,0}} \tilde{H} \Psi_{\nu_3} + y_{33} (\xi \sigma_1^* \bar{\Psi}_\ell)_{\mathbf{1}_{0,0}} \tilde{H} \Psi_{\nu_3} \right\} \delta(y - L) + \text{h.c.}
\end{aligned} \tag{12}$$

with $\tilde{H} \equiv \tau_2 H^* \tau_2$, and τ_i as the Pauli matrices. After electroweak and flavor spontaneous symmetry breaking, all leptons develop masses dictated by the above Yukawa interactions. The generated masses are modulated by the overlap of the relevant zero mode fermion profiles, the VEV profile of the Higgs, and the flavon VEVs given in Eqs. (10, 11).

From Eq. (12), The mass matrix m_l for charged leptons is

$$m_l = \frac{1}{(L \Lambda)^{\frac{3}{2}}} \frac{v_\varphi}{\Lambda} \frac{v}{\sqrt{2}} \sqrt{3} U_l \begin{pmatrix} \tilde{y}_e & 0 & 0 \\ 0 & \tilde{y}_\mu & 0 \\ 0 & 0 & \tilde{y}_\tau \end{pmatrix}, \tag{13}$$

where U_l stands for the so-called magic matrix

$$U_l = \frac{1}{\sqrt{3}} \begin{pmatrix} 1 & 1 & 1 \\ 1 & \omega & \omega^2 \\ 1 & \omega^2 & \omega \end{pmatrix}, \tag{14}$$

and $\tilde{y}_{e,\mu,\tau}$ are modified Yukawa couplings defined as

$$\tilde{y}_{e,\mu,\tau} = y_{e,\mu,\tau} F(0, c_\ell, c_{e_i}), \quad (15)$$

in terms of the overlapping function

$$\begin{aligned} F(y, c_L, c_R) &\equiv f_L^{(0)}(y, c_L) f_R^{(0)}(y, c_R) f_H(y) \\ &= \sqrt{\frac{2(1-\beta_H)(1-2c_L)(1+2c_R)k^3L^3}{[1-e^{-2(1-\beta_H)kL}][e^{(1-2c_L)kL}-1][e^{(1+2c_R)kL}-1]}} e^{-(1-\beta_H)kL} e^{(2-\beta_H-c_L+c_R)ky}. \end{aligned} \quad (16)$$

Given that $U_l^\dagger U_l = 1$, the diagonalization of the charged lepton mass matrix is straightforward, leading to charged lepton masses of the form

$$m_{e,\mu,\tau} = \frac{\sqrt{3}\tilde{y}_{e,\mu,\tau} v_\varphi v}{(L\Lambda)^{\frac{3}{2}} \Lambda \sqrt{2}}. \quad (17)$$

Analogously, taking into account the two distinct VEV alignments for the flavon triplet ξ in Eq. (10), the neutrino mass matrix for each respective case can be written as

$$m_\nu^{\text{I}} = \frac{1}{(L\Lambda')^{\frac{3}{2}}} \frac{v_\xi v}{\Lambda' \sqrt{2}} \begin{pmatrix} \tilde{y}_{11} \frac{v_{\sigma_1}}{\Lambda'} & 0 & \tilde{y}_{13} \frac{v_{\sigma_1}}{\Lambda'} \\ 0 & \tilde{y}_{22} \frac{v_{\sigma_2}}{\Lambda'} & 0 \\ \tilde{y}_{31} \frac{v_{\sigma_1}^*}{\Lambda'} & 0 & \tilde{y}_{33} \frac{v_{\sigma_1}^*}{\Lambda'} \end{pmatrix}, \quad (18)$$

$$m_\nu^{\text{II}} = \frac{1}{(L\Lambda')^{\frac{3}{2}}} \frac{v_\xi v}{\Lambda' \sqrt{2}} \sqrt{3} V_0 \begin{pmatrix} \tilde{y}_{11} \frac{v_{\sigma_1}}{\Lambda'} & 0 & \tilde{y}_{13} \frac{v_{\sigma_1}}{\Lambda'} \\ 0 & \tilde{y}_{22} \frac{v_{\sigma_2}}{\Lambda'} & 0 \\ \tilde{y}_{31} \frac{v_{\sigma_1}^*}{\Lambda'} & 0 & \tilde{y}_{33} \frac{v_{\sigma_1}^*}{\Lambda'} \end{pmatrix}, \quad (19)$$

with

$$\tilde{y}_{ij} = y_{ij} F(L, c_\ell, c_{\nu_j}), \quad (20)$$

and

$$V_0 \equiv \frac{1}{\sqrt{3}} \begin{pmatrix} \omega & 1 & 1 \\ 1 & \omega & 1 \\ 1 & 1 & \omega \end{pmatrix}. \quad (21)$$

Thus, the diagonalizing matrix for the neutrino sector can be parameterized as

$$U_\nu^{\text{I}} = \begin{pmatrix} \cos \theta_\nu & 0 & \sin \theta_\nu e^{i\varphi_\nu} \\ 0 & 1 & 0 \\ -\sin \theta_\nu e^{-i\varphi_\nu} & 0 & \cos \theta_\nu \end{pmatrix}, \quad (22)$$

$$U_\nu^{\text{II}} = V_0 \begin{pmatrix} \cos \theta_\nu & 0 & \sin \theta_\nu e^{i\varphi_\nu} \\ 0 & 1 & 0 \\ -\sin \theta_\nu e^{-i\varphi_\nu} & 0 & \cos \theta_\nu \end{pmatrix}. \quad (23)$$

In terms of the auxiliary functions

$$X_\nu^\pm = |\tilde{y}_{31}|^2 + |\tilde{y}_{33}|^2 \pm |\tilde{y}_{11}|^2 \pm |\tilde{y}_{13}|^2, \quad Y_\nu = \tilde{y}_{11}\tilde{y}_{33} - \tilde{y}_{13}\tilde{y}_{31}^*, \quad Z_\nu = \tilde{y}_{11}\tilde{y}_{31}^* + \tilde{y}_{13}\tilde{y}_{33}^*, \quad (24)$$

the relevant parameters of the model, θ_ν and φ_ν , are given by

$$\tan 2\theta_\nu = 2|Z_\nu|/X_\nu^-, \quad \varphi_\nu = \arg(v_{\sigma_1}^2 Z_\nu), \quad (25)$$

and the neutrino mass eigenvalues for both NH and IH are determined as

- Case I

$$\text{NH: } m_1 = \frac{\tilde{v}_1}{\sqrt{2}} M^-(X_\nu^+, Y_\nu), \quad m_2 = \tilde{v}_2 |\tilde{y}_{22}|, \quad m_3 = \frac{\tilde{v}_1}{\sqrt{2}} M^+(X_\nu^+, Y_\nu), \quad \text{for } X_\nu^- \cos 2\theta_\nu > 0, \quad (26)$$

$$\text{IH: } m_1 = \frac{\tilde{v}_1}{\sqrt{2}} M^+(X_\nu^+, Y_\nu), \quad m_2 = \tilde{v}_2 |\tilde{y}_{22}|, \quad m_3 = \frac{\tilde{v}_1}{\sqrt{2}} M^-(X_\nu^+, Y_\nu), \quad \text{for } X_\nu^- \cos 2\theta_\nu < 0, \quad (27)$$

- Case II

$$\text{NH: } m_1 = \sqrt{\frac{3}{2}} \tilde{v}_1 M^-(X_\nu^+, Y_\nu), \quad m_2 = \sqrt{3} \tilde{v}_2 |\tilde{y}_{22}|, \quad m_3 = \sqrt{\frac{3}{2}} \tilde{v}_1 M^+(X_\nu^+, Y_\nu), \quad \text{for } X_\nu^- \cos 2\theta_\nu > 0, \quad (28)$$

$$\text{IH: } m_1 = \sqrt{\frac{3}{2}} \tilde{v}_1 M^+(X_\nu^+, Y_\nu), \quad m_2 = \sqrt{3} \tilde{v}_2 |\tilde{y}_{22}|, \quad m_3 = \sqrt{\frac{3}{2}} \tilde{v}_1 M^-(X_\nu^+, Y_\nu), \quad \text{for } X_\nu^- \cos 2\theta_\nu < 0, \quad (29)$$

where we have defined

$$M^\pm(x, y) = \sqrt{x \pm \sqrt{x^2 - 4|y|^2}}, \quad (30)$$

and

$$\tilde{v}_\alpha = \left| \frac{1}{(L \Lambda')^{\frac{3}{2}}} \frac{v_\xi v_{\sigma_\alpha}}{\Lambda'} \frac{v}{\sqrt{2}} \right|, \quad \alpha = 1, 2. \quad (31)$$

Without loss of generality, the angle θ_ν is restricted to the interval $[0, \pi]$. Notice that $X_\nu^- \cos 2\theta_\nu = 2|Z_\nu| \cos^2 2\theta_\nu / \sin 2\theta_\nu$. As a result, for non-vanishing values of Z_ν , the neutrino mass spectrum displays Normal Hierarchy (NH) provided $0 < \theta_\nu < \pi/2$, whereas Inverted Hierarchy (IH) is realized for $\pi/2 < \theta_\nu < \pi$. The angle φ_ν , on the other hand, can take any value in the interval $[0, 2\pi]$.

At leading order, the lepton mixing matrix $U_{\text{PMNS}} = U_l^\dagger U_\nu$ becomes

$$U_{\text{PMNS}}^{\text{I}} = \frac{1}{\sqrt{3}} \begin{pmatrix} \cos \theta_\nu - e^{-i\varphi_\nu} \sin \theta_\nu & 1 & \cos \theta_\nu + e^{i\varphi_\nu} \sin \theta_\nu \\ \cos \theta_\nu - \omega e^{-i\varphi_\nu} \sin \theta_\nu & \omega^2 & \omega \cos \theta_\nu + e^{i\varphi_\nu} \sin \theta_\nu \\ \cos \theta_\nu - \omega^2 e^{-i\varphi_\nu} \sin \theta_\nu & \omega & \omega^2 \cos \theta_\nu + e^{i\varphi_\nu} \sin \theta_\nu \end{pmatrix}, \quad (32)$$

$$U_{\text{PMNS}}^{\text{II}} = \frac{-i\omega}{\sqrt{3}} \begin{pmatrix} \cos \theta_\nu - e^{-i\varphi_\nu} \sin \theta_\nu & 1 & \cos \theta_\nu + e^{i\varphi_\nu} \sin \theta_\nu \\ \omega \cos \theta_\nu - \omega^2 e^{-i\varphi_\nu} \sin \theta_\nu & 1 & \omega^2 \cos \theta_\nu + \omega e^{i\varphi_\nu} \sin \theta_\nu \\ \omega \cos \theta_\nu - e^{-i\varphi_\nu} \sin \theta_\nu & \omega^2 & \cos \theta_\nu + \omega e^{i\varphi_\nu} \sin \theta_\nu \end{pmatrix}. \quad (33)$$

In both cases, the solar, atmospheric and reactor angles can be written in terms of θ_ν and φ_ν as

$$\begin{aligned} \sin^2 \theta_{12} &= \frac{1}{2 - \sin 2\theta_\nu \cos \varphi_\nu}, \\ \sin^2 \theta_{23} &= \frac{1 - \sin 2\theta_\nu \sin(\pi/6 - \varphi_\nu)}{2 - \sin 2\theta_\nu \cos \varphi_\nu}, \\ \sin^2 \theta_{13} &= \frac{1}{3} (1 + \sin 2\theta_\nu \cos \varphi_\nu). \end{aligned} \quad (34)$$

A convenient description for the CP violating phase in this sector is the Jarlskog invariant $J_{\text{CP}} = \text{Im}[U_{e1}^* U_{\mu 3}^* U_{\mu 1} U_{e3}]$ [44], which in this parameterization takes the compact form

$$J_{\text{CP}} = -\frac{1}{6\sqrt{3}} \cos 2\theta_\nu. \quad (35)$$

It is worthy of attention the independence of J_{CP} upon φ_ν , and the simple predicted relation between the solar and reactor angles θ_{12} and θ_{13} :

$$\sin^2 \theta_{12} \cos^2 \theta_{13} = \frac{1}{3}. \quad (36)$$

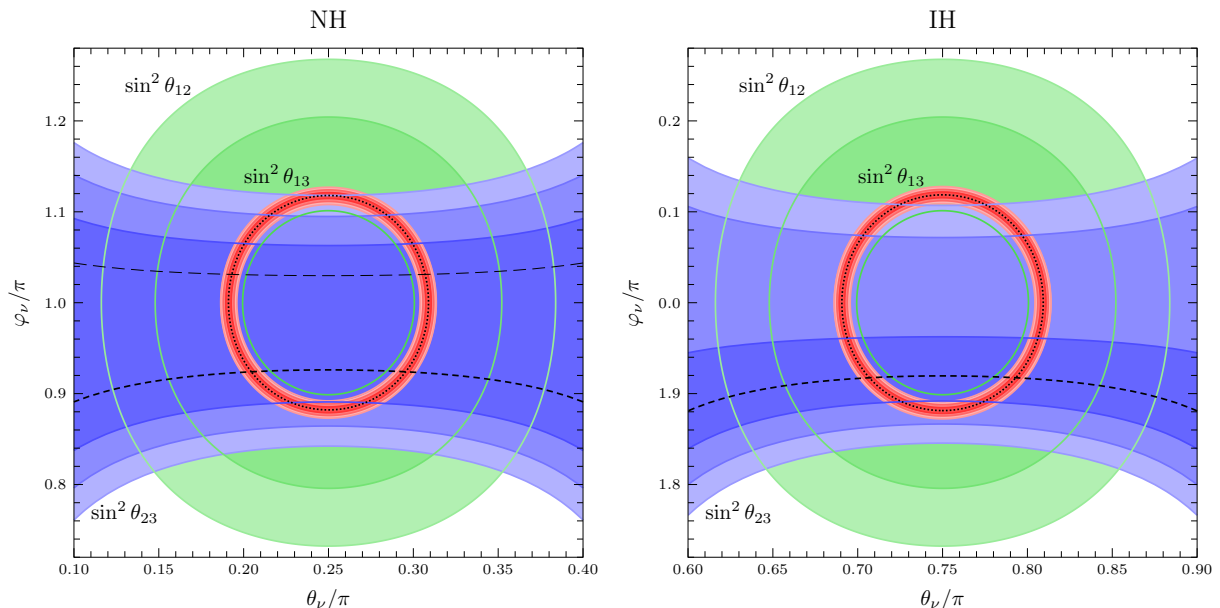


FIG. 1: 1σ , 2σ and 3σ ranges of $\sin^2 \theta_{12}$ (green), $\sin^2 \theta_{23}$ (blue) and $\sin^2 \theta_{13}$ (red) for normal (left panel) and inverted (right panel) neutrino mass hierarchies. Best-fit contours for $\sin^2 \theta_{13}$ ($\sin^2 \theta_{23}$) are indicated by dotted (short-dashed) lines. The long-dashed contour in the left panel represents the local minimum in the first octant of θ_{23} .

B. Phenomenological implications

As shown above, only two parameters are required to generate the three angles and the Dirac CP violating phase characterizing the lepton mixing matrix, making this model highly predictive. In the remaining part of this section we explore in detail the predictions for the lepton mixing parameters and the neutrino mass spectrum.

In Figure 1, the $\theta_\nu - \varphi_\nu$ parameter region compatible with experimental data is delimited using the global fit of neutrino oscillations given in [31] for each mass ordering, shown as the left and right hand panel. The model can reproduce successfully the best-fit values for the atmospheric and reactor angles, reaching simultaneously the 2σ region for the solar angle. The intersecting points of the “central” or best fit curve in the $\sin^2 \theta_{13}$ contour and the corresponding ones in the $\sin^2 \theta_{23}$ contour are located at

$$\begin{aligned}
 \text{NH}_1 : & \quad \theta_\nu/\pi = 0.204(0.296), & \quad \varphi_\nu/\pi = 0.924, \\
 \text{NH}_2 : & \quad \theta_\nu/\pi = 0.193(0.307), & \quad \varphi_\nu/\pi = 1.031, \\
 \text{IH} : & \quad \theta_\nu/\pi = 0.707(0.793), & \quad \varphi_\nu/\pi = 1.917,
 \end{aligned} \tag{37}$$

where NH_1 denotes the best-fit contour of $\sin^2 \theta_{23}$, and NH_2 corresponds to its local minimum in the first octant. Notice that the numbers in parenthesis denote the intersection values within the range $\theta_\nu \in [\pi/4, \pi/2] \cup [3\pi/4, \pi]$.

Once we have determined θ_ν and φ_ν from the central values of the atmospheric and reactor oscillation global fits, the predictions for the solar angle and the Jarlskog invariant can be straightforwardly obtained using Eqs. (34, 35). For completeness, in Table II we present the full set of mixing parameters derived from the points defined in Eq. (37).

Remarkably, the central prediction for $\sin^2 \theta_{12}$ falls very close to its 1σ boundary. In addition, notice that the 1σ range of J_{CP} is entirely contained in the region $\theta_\nu \in [0, \pi/4] \cup [3\pi/4, \pi]$.

We conclude this section bringing forth a consistent realization of lepton masses and mixing angles. In the numerical analysis, we assume that the fundamental 5D scale is $k \simeq \Lambda \simeq M_{\text{Pl}}$, with $M_{\text{Pl}} \simeq 2.44 \times 10^{18}$ GeV as the reduced Planck mass. We also set the scale $\Lambda' \simeq k' = ke^{-kL} \simeq 1.5$ TeV in order to account for the hierarchy between the Planck and the electroweak scales, allowing for the lowest KK gauge boson resonances (with masses $m_{KK} = 3 \sim 4$ TeV) to be within reach of the LHC experiments. The Higgs VEV is identified with its standard model value $v \simeq 246$

	NH ₁	NH ₂	IH
$\sin^2 \theta_{23}/10^{-1}$	5.67	4.73	5.73
$\sin^2 \theta_{13}/10^{-2}$	2.26	2.26	2.29
$\sin^2 \theta_{12}/10^{-1}$	3.41	3.41	3.41
$J_{CP}/10^{-2}$	-(+)2.71	-(+)3.37	+(-)2.57

TABLE II: Central predictions for $\sin^2 \theta_{12}$ and J_{CP} obtained from the central values of the atmospheric and reactor angles reported in Ref. [31]. The sign of J_{CP} in the parentheses corresponds to the bracketed prediction for θ_ν in Eq. (37).

GeV, and the ratios v_φ/Λ , v_ξ/Λ' , v_{σ_1}/Λ' , v_{σ_2}/Λ' , are all fixed to 0.1 (thus considering real-valued flavon VEVs). The Higgs localization parameter β , common to all mass matrix elements, is chosen as 0.95 in the following discussion.

As an illustrative example, we can choose $c_\ell = 1.85$, $c_e = -0.27$, $c_\mu = -0.44$, $c_\tau = -0.71$, $|y_e| = 0.861$, $|y_\mu| = 0.898$, $|y_\tau| = 0.994$ to generate the charged lepton masses $m_e = 0.511$ MeV, $m_\mu = 105.7$ MeV, $m_\tau = 1.777$ GeV. For the neutrino sector, benchmark points (BPs) in parameter space are given in Table III. There, the four BPs are labeled according to their hierarchy scheme and case as NH-I, NH-II, IH-I, IH-II. One sees that, indeed, the large disparity between charged lepton masses is reproduced for Yukawa couplings of the same order of magnitude.

	NH-I	NH-II	IH-I	IH-II
c_{ν_1}	-1.40	-1.41	-1.39	-1.40
c_{ν_2}	-1.38	-1.40	-1.33	-1.35
c_{ν_3}	-1.34	-1.36	-1.34	-1.36
y_{11}	$-1.000 - 0.307i$	$0.282 + 1.166i$	$0.752 + 0.096i$	$-0.674 + 0.520i$
y_{13}	$-0.451 + 0.631i$	$0.031 - 0.880i$	$0.919 - 0.432i$	$1.026 - 0.542i$
y_{22}	$0.860 + 0.353i$	$0.097 - 1.088i$	$-0.905 - 0.194i$	$0.974 + 0.431i$
y_{31}	$0.667 + 0.397i$	$0.001 - 0.881i$	$0.941 + 0.383i$	$-1.070 + 0.450i$
y_{33}	$0.792 - 0.683i$	$-0.324 + 1.154i$	$0.746 - 0.136i$	$0.829 - 0.191i$

TABLE III: Benchmark points for the neutrino sector, featuring both NH and IH in Cases I and II.

The neutrino masses, splittings and mixing angles associated to each BP are displayed in Table IV. All the obtained neutrino oscillation parameters are consistent with the global fit in Ref. [31]. In particular, the reproduced atmospheric and reactor angles lie comfortably in their respective 1σ region, whereas the solar angle values are contained in the 2σ range, very close to the 1σ boundary.

	NH-I	NH-II	IH-I	IH-II
m_1 [eV]	1.80×10^{-3}	2.59×10^{-3}	4.88×10^{-2}	4.89×10^{-2}
m_2 [eV]	8.90×10^{-3}	9.10×10^{-3}	4.96×10^{-2}	4.97×10^{-2}
m_3 [eV]	4.98×10^{-2}	4.99×10^{-2}	2.41×10^{-3}	3.50×10^{-3}
$\Delta m_{21}^2 [10^{-5} \text{eV}^2]$	7.60	7.60	7.50	7.48
$ \Delta m_{31}^2 [10^{-3} \text{eV}^2]$	2.48	2.48	2.38	2.38
$\sin^2 \theta_{12}/10^{-1}$	3.41	3.41	3.41	3.41
$\sin^2 \theta_{23}/10^{-1}$	5.67	5.67	5.73	5.73
$\sin^2 \theta_{13}/10^{-2}$	2.26	2.26	2.29	2.29
$J_{CP}/10^{-2}$	-2.71	-2.71	-2.58	-2.57

TABLE IV: Neutrino masses and oscillation parameters associated to the four chosen benchmark points.

IV. QUARK SECTOR

Field	Ψ_U	Ψ_C	Ψ_T	Ψ_u	Ψ_c	Ψ_t	Ψ_d	Ψ_s	Ψ_b
$\Delta(27)$	$\mathbf{1}_{0,2}$	$\mathbf{1}_{0,1}$	$\mathbf{1}_{0,0}$	$\mathbf{1}_{0,2}$	$\mathbf{1}_{0,0}$	$\mathbf{1}_{0,2}$	$\mathbf{1}_{0,1}$	$\mathbf{1}_{0,0}$	$\mathbf{1}_{0,1}$
Z_4	$-i$	$-i$	$-i$	1	1	$-i$	1	$-i$	$-i$
Z'_4	1	1	1	-1	-1	-1	-1	-1	-1

TABLE V: Particle content and transformation properties of the quark sector under the flavor symmetry $\Delta(27) \otimes Z_4 \otimes Z'_4$.

The quark transformation properties under the family group $\Delta(27) \otimes Z_4 \otimes Z'_4$ are given in Table V. At leading order, the most general invariant Yukawa interactions can be written as

$$\begin{aligned} \mathcal{L}_Y^q = \frac{\sqrt{G}}{(\Lambda')^{\frac{5}{2}}} & \left\{ y_{uu}\sigma_2^* \bar{\Psi}_U \tilde{H} \Psi_u + y_{ct}\sigma_1^* \bar{\Psi}_C \tilde{H} \Psi_t + y_{tc}\sigma_2^* \bar{\Psi}_T \tilde{H} \Psi_c + y_{tt}\sigma_1 \bar{\Psi}_T \tilde{H} \Psi_t \right. \\ & + y_{ds}\sigma_1^* \bar{\Psi}_U H \Psi_s + y_{db}\sigma_1 \bar{\Psi}_U H \Psi_b + y_{sd}\sigma_2^* \bar{\Psi}_C H \Psi_d \\ & \left. + y_{ss}\sigma_1 \bar{\Psi}_C H \Psi_s + y_{bb}\sigma_1^* \bar{\Psi}_T H \Psi_b \right\} \delta(y-L) + \text{h.c.} \end{aligned} \quad (38)$$

Again, after spontaneous electroweak and flavor symmetry breaking, the mass matrices for the up and down quark sectors read

$$\begin{aligned} m^u &= \frac{1}{(L\Lambda')^{\frac{3}{2}}} \frac{v}{\sqrt{2}} \begin{pmatrix} \tilde{y}_{uu}v_{\sigma_2}^*/\Lambda' & 0 & 0 \\ 0 & 0 & \tilde{y}_{ct}v_{\sigma_1}^*/\Lambda' \\ 0 & \tilde{y}_{tc}v_{\sigma_2}^*/\Lambda' & \tilde{y}_{tt}v_{\sigma_1}/\Lambda' \end{pmatrix}, \\ m^d &= \frac{1}{(L\Lambda')^{\frac{3}{2}}} \frac{v}{\sqrt{2}} \begin{pmatrix} 0 & \tilde{y}_{ds}v_{\sigma_1}^*/\Lambda' & \tilde{y}_{db}v_{\sigma_1}/\Lambda' \\ \tilde{y}_{sd}v_{\sigma_2}^*/\Lambda' & \tilde{y}_{ss}v_{\sigma_1}/\Lambda' & 0 \\ 0 & 0 & \tilde{y}_{bb}v_{\sigma_1}^*/\Lambda' \end{pmatrix}. \end{aligned} \quad (39)$$

where

$$\begin{aligned} \tilde{y}_{u_i u_j} &= y_{u_i u_j} F(L, c_{Q_i}, c_{u_j}), \\ \tilde{y}_{d_i d_j} &= y_{d_i d_j} F(L, c_{Q_i}, c_{d_j}). \end{aligned} \quad (40)$$

The up-type quark mass matrix is already block-diagonal. The diagonalization of the down-type mass matrix m^d requires a more careful treatment. For the sake of simplicity, in the following analysis we denote the ij element of m^u (m^d) as m_{ij}^u (m_{ij}^d). The product of the down-type mass matrix and its adjoint

$$m^d m^{d\dagger} = \begin{pmatrix} |m_{12}^d|^2 + |m_{13}^d|^2 & m_{12}^d m_{22}^{d*} & m_{13}^d m_{33}^{d*} \\ m_{12}^{d*} m_{22}^d & |m_{21}^d|^2 + |m_{22}^d|^2 & 0 \\ m_{13}^{d*} m_{33}^d & 0 & |m_{33}^d|^2 \end{pmatrix} \quad (41)$$

can be diagonalized in two steps: in first place, an approximate block diagonalization

$$U^{d\dagger} m^d m^{d\dagger} U^{d'} \simeq \begin{pmatrix} |m_{12}^d|^2 & m_{12}^d m_{22}^{d*} & 0 \\ m_{12}^{d*} m_{22}^d & |m_{21}^d|^2 + |m_{22}^d|^2 & 0 \\ 0 & 0 & |m_{33}^d|^2 \end{pmatrix}, \quad (42)$$

is accomplished with the aid of the transformation matrix

$$U^{d'} \simeq \begin{pmatrix} 1 & 0 & \epsilon \\ 0 & 1 & 0 \\ -\epsilon^* & 0 & 1 \end{pmatrix}, \quad (43)$$

and subsequently the diagonalization is completed through a unitary rotation of the upper block. This approximation is consistent provided $|m_{33}^d| \gg |m_{12}^d|, |m_{13}^d|, |m_{22}^d|$ and $|\epsilon| \ll 1$. The resulting diagonalization matrices for the up and down sectors can be parameterized as

$$U_u = \begin{pmatrix} 1 & 0 & 0 \\ 0 & \cos \theta_u & \sin \theta_u e^{i\varphi_u} \\ 0 & -\sin \theta_u e^{-i\varphi_u} & \cos \theta_u \end{pmatrix}, \quad (44)$$

$$U_d \simeq \begin{pmatrix} \cos \theta_d & \sin \theta_d e^{i\varphi_d} & \epsilon \\ -\sin \theta_d e^{-i\varphi_d} & \cos \theta_d & 0 \\ -\epsilon^* \cos \theta_d & -\epsilon^* \sin \theta_d e^{i\varphi_d} & 1 \end{pmatrix},$$

with

$$\begin{aligned} \tan 2\theta_u &= 2|Z_u|/X_u^-, & \varphi_u &= \arg Z_u, \\ \tan 2\theta_d &= 2|Z_d|/X_d^-, & \varphi_d &= \arg Z_d, & \epsilon &= B_d/A_d, \end{aligned} \quad (45)$$

and

$$\begin{aligned} X_u^\pm &= |m_{33}^u|^2 + |m_{32}^u|^2 \pm |m_{23}^u|^2, & Y_u &= m_{23}^u m_{32}^{u*}, & Z_u &= m_{23}^u m_{33}^{u*}, \\ X_d^\pm &= |m_{22}^d|^2 + |m_{21}^d|^2 \pm |m_{12}^d|^2, & Y_d &= m_{12}^d m_{21}^{d*}, & Z_d &= m_{12}^d m_{22}^{d*}, \\ A_d &= |m_{33}^d|^2 - |m_{12}^d|^2 - |m_{13}^d|^2, & B_d &= m_{13}^d m_{33}^{d*}. \end{aligned} \quad (46)$$

Correspondingly, the quark mass eigenvalues can be expressed in terms of M^\pm , defined in Eq. (30), as

$$\begin{aligned} m_u &= |m_{11}^u|, & m_c &= \frac{1}{\sqrt{2}} M^-(X_u^+, Y_u), & m_t &= \frac{1}{\sqrt{2}} M^+(X_u^+, Y_u), \\ m_d &= \frac{1}{\sqrt{2}} M^-(X_d^+, Y_d), & m_s &= \frac{1}{\sqrt{2}} M^+(X_d^+, Y_d), & m_b &= |m_{33}^b|, \end{aligned} \quad (47)$$

so that the CKM matrix is given by

$$\begin{aligned} V_{\text{CKM}} &= U_u^\dagger U_d \\ &\simeq \begin{pmatrix} \cos \theta_d & e^{i\varphi_d} \sin \theta_d & \epsilon \\ -e^{-i\varphi_d} \cos \theta_u \sin \theta_d - e^{i\varphi_u} \sin \theta_u \cos \theta_d \epsilon^* & \cos \theta_d \cos \theta_u - e^{i(\varphi_u + \varphi_d)} \sin \theta_u \sin \theta_d \epsilon^* & -e^{i\varphi_u} \sin \theta_u \\ -e^{-i(\varphi_d + \varphi_u)} \sin \theta_d \sin \theta_u - \cos \theta_u \cos \theta_d \epsilon^* & e^{-i\varphi_u} \cos \theta_d \sin \theta_u - e^{i\varphi_d} \cos \theta_u \sin \theta_d \epsilon^* & \cos \theta_u \end{pmatrix}. \end{aligned} \quad (48)$$

Hence, the quark sector Dirac CP phase (in PDG convention) and the Jarlskog invariant take the form

$$\delta_{\text{CP}}^q = \pi - \arg(\epsilon) + \varphi_d + \varphi_u, \quad (49)$$

$$J_{\text{CP}}^q \simeq \frac{1}{4} |\epsilon| \sin 2\theta_d \sin 2\theta_u \sin \delta_{\text{CP}}^q. \quad (50)$$

According to Eq. (40), the size of up and down mass matrix elements is determined by the overlap of the 5D quark field zero mode profiles, *i.e.*, $m_{ij}^u \propto f_L^{(0)}(L, c_{Q_i}) f_R^{(0)}(L, c_{u_j})$ and $m_{ij}^d \propto f_L^{(0)}(L, c_{Q_i}) f_R^{(0)}(L, c_{d_j})$. If the wave function localization parameters $c_{Q_i}, c_{u_i}, c_{d_i}$ are chosen such that the quark zero mode profiles obey

$$\begin{aligned} f_L^{(0)}(L, c_U) &\ll f_L^{(0)}(L, c_C) \ll f_L^{(0)}(L, c_T), \\ f_R^{(0)}(L, c_u) &\ll f_R^{(0)}(L, c_c) \ll f_R^{(0)}(L, c_t), \\ f_R^{(0)}(L, c_d) &\ll f_R^{(0)}(L, c_s) \ll f_R^{(0)}(L, c_b), \end{aligned} \quad (51)$$

then the elements of m^u and m^d approximately satisfy

$$m_{11}^u \ll m_{23}^u \sim m_{32}^u \ll m_{33}^u, \quad m_{12}^d \sim m_{21}^d \ll m_{22}^d \ll m_{33}^d, \quad m_{13}^d \ll m_{33}^d, \quad (52)$$

justifying the perturbative diagonalization performed on $m^d m^{d\dagger}$. These relations imply that $X_{u,d}^+ \gg |Y_{u,d}|$ holds, and therefore, a rough estimate for the mixing parameters and quark mass spectrum is

$$\begin{aligned} \theta_u &\sim \left| \frac{m_{23}^u}{m_{33}^u} \right| \sim \frac{f_L^{(0)}(L, c_C)}{f_L^{(0)}(L, c_T)}, & \theta_d &\sim \left| \frac{m_{12}^d}{m_{22}^d} \right| \sim \frac{f_L^{(0)}(L, c_U)}{f_L^{(0)}(L, c_C)}, & |\epsilon| &\sim \left| \frac{m_{13}^d}{m_{33}^d} \right| \sim \frac{f_L^{(0)}(L, c_U)}{f_L^{(0)}(L, c_T)}, \\ m_u &\sim |m_{11}^u|, & m_c &\sim \left| \frac{m_{23}^u m_{32}^u}{m_{33}^u} \right|, & m_t &\sim |m_{33}^u|, \\ m_d &\sim \left| \frac{m_{12}^d m_{21}^d}{m_{22}^d} \right|, & m_s &\sim |m_{22}^d|, & m_b &\sim |m_{33}^d|. \end{aligned} \quad (53)$$

Thus, in order to reproduce plausible quark masses and mixings, namely:

$$\begin{aligned} \theta_u &\sim 10^{-1}, & \theta_d &\sim 10^{-2}, & |\epsilon| &\sim 10^{-3}, \\ m_u : m_c : m_t &\sim 10^{-5} : 10^{-2} : 1, \\ m_d : m_s : m_b &\sim 10^{-3} : 10^{-2} : 1, \end{aligned} \quad (54)$$

the quark zero mode profiles must observe the following hierarchy:

$$\begin{aligned} f_L^{(0)}(L, c_U) : f_L^{(0)}(L, c_C) : f_L^{(0)}(L, c_T) &\sim 10^{-3} : 10^{-1} : 1, \\ f_R^{(0)}(L, c_u) : f_R^{(0)}(L, c_c) : f_R^{(0)}(L, c_t) &\sim 10^{-2} : 10^{-1} : 1, \\ f_R^{(0)}(L, c_d) : f_R^{(0)}(L, c_s) : f_R^{(0)}(L, c_b) &\sim 10^{-1} : 10^{-1} : 1. \end{aligned} \quad (55)$$

To conclude this section, an explicit realization of quark masses and mixings is presented. The choice $c_U = 1.97$, $c_C = 1.92$, $c_T = 1.83$, $c_u = -0.76$, $c_c = -0.62$, $c_t = -0.56$, $c_d = -0.74$, $c_s = -0.69$, $c_b = -0.68$, $y_{uu} = -0.438 - 0.954i$, $y_{ct} = -0.360 - 1.038i$, $y_{tc} = 1.147 - 0.273i$, $y_{tt} = -0.372 - 1.073i$, $y_{ds} = -0.966 - 0.285i$, $y_{db} = 0.290 + 0.400i$, $y_{sd} = 0.838 - 0.226i$, $y_{ss} = -0.703 - 0.207i$, $y_{bb} = 0.637 - 0.879i$, generates the quark mass spectrum

$$\begin{aligned} m_u &= 2.30 \text{ MeV}, & m_c &= 1.275 \text{ GeV}, & m_t &= 173 \text{ GeV}, \\ m_d &= 4.80 \text{ MeV}, & m_s &= 95.0 \text{ MeV}, & m_b &= 4.18 \text{ GeV}, \end{aligned} \quad (56)$$

and fixes the magnitude of V_{CKM} elements at

$$|V_{CKM}| = \begin{pmatrix} 0.974 & 0.225 & 0.0035 \\ 0.225 & 0.973 & 0.0414 \\ 0.0089 & 0.041 & 0.999 \end{pmatrix}. \quad (57)$$

Finally, the obtained values for the Dirac CP phase and the Jarlskog invariant are

$$\delta_{CP}^q = 1.25, \quad J_{CP}^q = 3.06 \times 10^{-5}. \quad (58)$$

The resulting quark masses and mixings are consistent with the current experimental data [1], and the precision of the results can be improved by incorporating high order corrections, addressed in the next section.

V. HIGH ORDER CORRECTIONS

From the particle content and above transformation properties, one finds that nontrivial high order corrections to the charged lepton sector are absent in the present model. The next-to-leading order (NLO) corrections to the neutrino Yukawa interactions are given by

$$\delta \mathcal{L}_Y^\nu = \sqrt{G} \frac{x_2}{(\Lambda')^{\frac{9}{2}}} [(\xi^* \xi^*)_{\mathbf{3}} \sigma_2^* \bar{\Psi}_l]_{\mathbf{1}_{0,0}} \tilde{H} \Psi_{\nu 2} \delta(y - L) + \text{h.c.} \quad (59)$$

However, the contribution of these terms to the neutrino masses and mixing parameters can be absorbed by a proper redefinition of the parameter y_{22} after SSB. Hence, in order to estimate the effects of higher order corrections in this

sector, we need to investigate the Yukawa terms involving an additional $(v_{\text{IR}}/\Lambda')^2$ suppression with respect to the lowest order terms in Eq. (12), where we have introduced v_{IR} to characterize the magnitude of $v_\xi \sim v_{\sigma_1} \sim v_{\sigma_2}$.

The contraction of the field products $\bar{\Psi}_l \tilde{H} \Psi_{\nu_1}$, $\bar{\Psi}_l \tilde{H} \Psi_{\nu_3}$, transforming as $(\bar{\mathbf{3}}, -1, -1)$ under $\Delta(27) \otimes Z_4 \otimes Z'_4$, with the flavon operators

$$\frac{1}{(\Lambda')^{\frac{11}{2}}} (\xi \xi^*)_{\mathbf{1}_{a,2}} \xi \sigma_1, \quad \frac{1}{(\Lambda')^{\frac{11}{2}}} (\xi \xi^*)_{\mathbf{1}_{a,1}} \xi \sigma_1^*, \quad \frac{1}{(\Lambda')^{\frac{11}{2}}} \xi \sigma_1^3, \quad \frac{1}{(\Lambda')^{\frac{11}{2}}} \xi \sigma_1^{*3}, \quad (60)$$

as well as the combination of $\bar{\Psi}_l \tilde{H} \Psi_{\nu_2} \sim (\bar{\mathbf{3}}, i, -1)$ and

$$\frac{1}{(\Lambda')^{\frac{11}{2}}} (\xi \xi^*)_{\mathbf{1}_{a,b}} \xi \sigma_2, \quad \frac{1}{(\Lambda')^{\frac{11}{2}}} \xi \sigma_1^2 \sigma_2, \quad \frac{1}{(\Lambda')^{\frac{11}{2}}} \xi \sigma_1^{*2} \sigma_2, \quad (61)$$

provide the desired high order corrections to the neutrino Yukawa interactions. In the above expressions, the indices $a, b = 0, 1, 2$ label the different singlets of $\Delta(27)$. Additional terms that can be absorbed into y_{11} , y_{13} , y_{22} , y_{31} and y_{33} have been omitted. Taking into consideration these corrections, the neutrino mass matrix m_ν can be roughly written as

$$m_\nu \simeq \frac{1}{(L \Lambda')^{\frac{3}{2}} \sqrt{2}} \left[\frac{v_\xi}{\Lambda'} \begin{pmatrix} \tilde{y}_{11} \frac{v_{\sigma_1}}{\Lambda'} & 0 & \tilde{y}_{13} \frac{v_{\sigma_1}}{\Lambda'} \\ 0 & \tilde{y}_{22} \frac{v_{\sigma_2}}{\Lambda'} & 0 \\ \tilde{y}_{31} \frac{v_{\sigma_1}^*}{\Lambda'} & 0 & \tilde{y}_{33} \frac{v_{\sigma_1}^*}{\Lambda'} \end{pmatrix} + \left(\frac{v_{\text{IR}}}{\Lambda'} \right)^4 \begin{pmatrix} 0 & \tilde{x}_{12} & 0 \\ \tilde{x}_{21} & 0 & \tilde{x}_{23} \\ 0 & \tilde{x}_{32} & 0 \end{pmatrix} \right], \quad (62)$$

with $\tilde{x}_{ij} = x_{ij} F(L, c_l, c_{\nu_j})$, and x_{ij} as dimensionless parameters of order $O(1)$.

Working under the same numerical framework established in Section III, one can readily estimate the shift in the neutrino oscillation parameters induced by high order corrections of the Yukawa interaction. Particularly, in Case I, taking x_{ij} as random complex numbers with magnitudes ranging from 2 to 6, and $v_{\text{IR}} = 0.1$, the resulting deviations in the neutrino mixing parameters with respect to their LO values can be estimated as

$$\delta s_{12}^2 \sim 0.01 \quad \delta s_{23}^2 \sim 0.01 \quad \delta s_{13}^2 \sim 0.001 \quad \delta J_{CP} \sim 0.001. \quad (63)$$

On the other hand, the corrections to the neutrino mass splittings are negligible

$$\delta (\Delta m_{21}^2) \sim 10^{-7} \text{ eV}^2, \quad \delta (\Delta |m_{31}^2|) \sim 10^{-6} \text{ eV}^2. \quad (64)$$

From Eq. (63), it is clear that high order corrections can easily drive s_{12}^2 into its 1σ region while keeping the remaining parameters optimal.

Turning to the quark sector, every bilinear formed by $\bar{\Psi}_{Q_i}$ and Ψ_{u_i} or Ψ_{d_i} can produce a high order correction to the Yukawa interaction whenever it is contracted with the adequate cubic flavon operator. Beside terms that can be absorbed by a redefinition of $y_{u_i u_j}$ or $y_{d_i d_j}$ in Eq. (38), all the NLO contributions can be classified into three categories:

- Invariant products of $\bar{\Psi}_U \tilde{H} \Psi_c$, $\bar{\Psi}_C \tilde{H} \Psi_u$, $\bar{\Psi}_T H \Psi_d \sim (\mathbf{1}_{0,1}, i, -1)$ with

$$\frac{1}{(\Lambda')^{\frac{9}{2}}} (\xi \xi^*)_{\mathbf{1}_{0,2}} \sigma_2^*, \quad \frac{1}{(\Lambda')^{\frac{9}{2}}} \sigma_1^2 \sigma_2^*. \quad (65)$$

- Invariant products of $\bar{\Psi}_U \tilde{H} \Psi_t$, $\bar{\Psi}_C H \Psi_b$, $\bar{\Psi}_T H \Psi_s \sim (\mathbf{1}_{0,0}, 1, -1)$ with

$$\frac{1}{(\Lambda')^{\frac{9}{2}}} (\xi \xi^*)_{\mathbf{1}_{0,2}} \sigma_1, \quad \frac{1}{(\Lambda')^{\frac{9}{2}}} (\xi \xi^*)_{\mathbf{1}_{0,1}} \sigma_1^*, \quad \frac{1}{(\Lambda')^{\frac{9}{2}}} \sigma_1^3, \quad \frac{1}{(\Lambda')^{\frac{9}{2}}} \sigma_1^{*3}. \quad (66)$$

- Invariant products of $\bar{\Psi}_C \tilde{H} \Psi_c$, $\bar{\Psi}_T \tilde{H} \Psi_u$ and $\bar{\Psi}_U H \Psi_d \sim (\mathbf{1}_{0,2}, i, -1)$ with

$$\frac{1}{(\Lambda')^{\frac{9}{2}}} (\xi \xi^*)_{\mathbf{1}_{0,1}} \sigma_2^*, \quad \frac{1}{(\Lambda')^{\frac{9}{2}}} \sigma_1^{*2} \sigma_2^*. \quad (67)$$

Again, after symmetry breaking, the quark mass matrices m_u and m_d can be approximately written as

$$\begin{aligned}
m^u &= \frac{1}{(L\Lambda')^{\frac{3}{2}}\sqrt{2}} \left[\begin{pmatrix} \tilde{y}_{uu}v_{\sigma_2}^*/\Lambda' & 0 & 0 \\ 0 & 0 & \tilde{y}_{ct}v_{\sigma_1}^*/\Lambda' \\ 0 & \tilde{y}_{tc}v_{\sigma_2}^*/\Lambda' & \tilde{y}_{tt}v_{\sigma_1}/\Lambda' \end{pmatrix} + \left(\frac{v_{\text{IR}}}{\Lambda'}\right)^3 \begin{pmatrix} 0 & \tilde{x}_{uc} & \tilde{x}_{ut} \\ \tilde{x}_{cu} & \tilde{x}_{cc} & 0 \\ \tilde{x}_{tu} & 0 & 0 \end{pmatrix} \right], \\
m^d &= \frac{1}{(L\Lambda')^{\frac{3}{2}}\sqrt{2}} \left[\begin{pmatrix} 0 & \tilde{y}_{ds}v_{\sigma_1}^*/\Lambda' & \tilde{y}_{db}v_{\sigma_1}/\Lambda' \\ \tilde{y}_{sd}v_{\sigma_2}^*/\Lambda' & \tilde{y}_{ss}v_{\sigma_1}/\Lambda' & 0 \\ 0 & 0 & \tilde{y}_{bb}v_{\sigma_1}/\Lambda' \end{pmatrix} + \left(\frac{v_{\text{IR}}}{\Lambda'}\right)^3 \begin{pmatrix} \tilde{x}_{dd} & 0 & 0 \\ 0 & 0 & \tilde{x}_{sb} \\ \tilde{x}_{bd} & \tilde{x}_{bs} & 0 \end{pmatrix} \right]. \quad (68)
\end{aligned}$$

Here we have defined $\tilde{x}_{u_i u_j} = x_{u_i u_j} F(L, c_{Q_i}, c_{u_j})$ and $\tilde{x}_{d_i d_j} = x_{d_i d_j} F(L, c_{Q_i}, c_{d_j})$, where the couplings $x_{u_i u_j}$ and $x_{d_i d_j}$ represent dimensionless parameters of order $O(1)$. As a numerical example, taking $x_{u_i u_j}$, $x_{d_i d_j}$ as random complex numbers with magnitudes ranging from 1 to 4 for x_{uc} , x_{cu} , x_{bd} , x_{cc} , x_{tu} , x_{dd} , and from 2 to 6 for x_{ut} , x_{sb} , x_{bs} , while keeping the values of c_{Q_i} , c_{u_i} , c_{d_i} , $y_{u_i u_j}$ and $y_{d_i d_j}$ reported in Section IV, the order of deviation with respect to the LO values of the quark masses is

$$\begin{aligned}
\delta m_u &\sim 0.001 \text{ MeV}, & \delta m_c &\sim 10 \text{ MeV}, & \delta m_t &\sim 0.1 \text{ MeV}, \\
\delta m_d &\sim 0.1 \text{ MeV}, & \delta m_s &\sim 0.1 \text{ MeV}, & \delta m_b &\sim 0.5 \text{ MeV}. \quad (69)
\end{aligned}$$

The corresponding correction to the first order CKM matrix is of order

$$\delta |V_{\text{CKM}}| \sim \begin{pmatrix} 0.001 & 0.005 & 0.0001 \\ 0.005 & 0.001 & 0.001 \\ 0.0005 & 0.001 & 0.00005 \end{pmatrix}, \quad (70)$$

and the values for the quark CP violating phase and the Jarlskog invariant are displaced by

$$\delta(\delta_{\text{CP}}^q) \sim 0.1, \quad \delta J_{\text{CP}}^q \sim 10^{-6}. \quad (71)$$

As for the lepton sector, it is not difficult to find parameter values reproducing the quark mass and mixing parameters required to fit the current experimentally observed values.

VI. CONCLUSIONS

We have proposed a five-dimensional warped model in which all standard model fields propagate into the bulk. Its structure is summarized in the ‘‘cartoon’’ depicted in Figure 2. Mass hierarchies in principle arise from an adequate choice of the bulk shape parameters, while fermion mixing angles are constrained by relations which follow from the postulated $\Delta(27)$ flavor symmetry group, broken on the branes by a set of flavon fields. The neutrino mixing parameters and the Dirac CP violation phase are described in terms of just two independent parameters at leading order. This leads to stringent predictions for the lepton mixing matrix which should be tested in future neutrino oscillation experiments. Likewise the scheme also includes the quark sector, providing an adequate description of the quark mixing matrix. The effect of next-to-leading order contributions is estimated to be fully consistent with the experimental requirements.

Acknowledgements

This work is supported by the National Natural Science Foundation of China under Grant Nos. 11275188, 11179007 and 11522546; by the Spanish grants FPA2014-58183-P, Multidark CSD2009-00064, SEV-2014-0398 (MINECO) and PROMETEOII/2014/084 (Generalitat Valenciana). A.D.R. and C.A.V-A. acknowledge support from CONACyT (Mexico), grants 250610 and 251357.

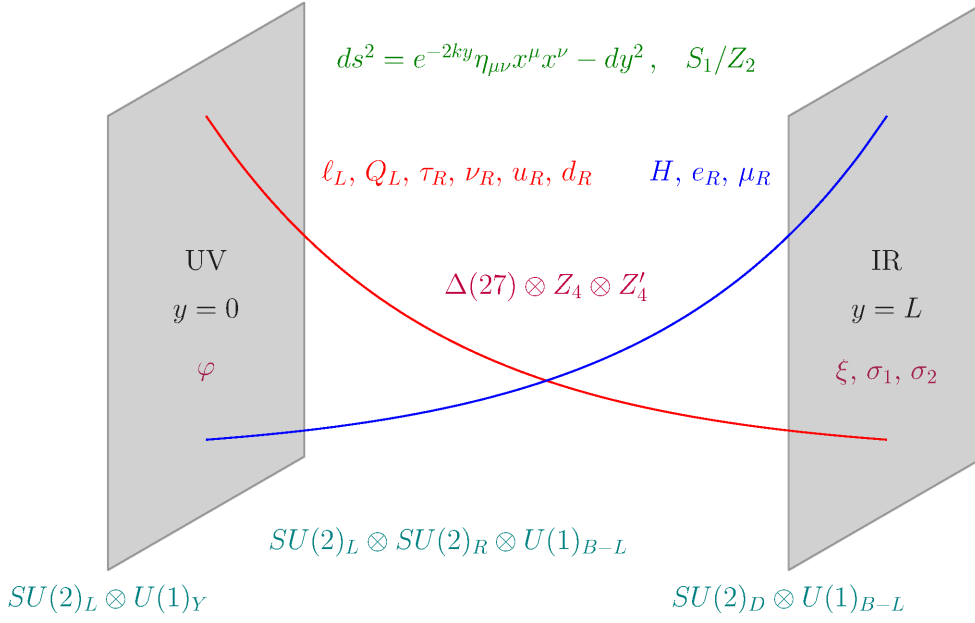


FIG. 2: Pictorial description of the basic warped model structure, showing the UV (IR) peaked nature of the standard model fields.

Appendix A: Group theory of $\Delta(27)$ and its representation

The $\Delta(27)$ group is isomorphic to $(Z_3 \otimes Z_3) \rtimes Z_3$. It can be conveniently expressed in terms of three generators a , a' and b which satisfy the following relations:

$$\begin{aligned} a^3 = a'^3 = b^3 = 1, & \quad aa' = a'a, \\ bab^{-1} = a^{-1}a'^{-1}, & \quad ba'b^{-1} = a. \end{aligned} \quad (\text{A1})$$

All $\Delta(27)$ elements can be written into the form $b^k a^m a'^n$, with $k, m, n = 0, 1, 2$. The group has 11 conjugacy classes, given by

$$\begin{aligned} 1C_1 &= \{1\}, \\ 1C_1^{(1)} &= \{aa'^2\}, \\ 1C_1^{(2)} &= \{a^2a'\}, \\ 3C_3^{(0,1)} &= \{a, a', a^2a'^2\}, \\ 3C_3^{(0,2)} &= \{a^2, a'^2, aa'\}, \\ 3C_3^{(1,0)} &= \{b, baa'^2, ba^2a'\}, \\ 3C_3^{(1,1)} &= \{ba, ba', ba^2a'^2\}, \\ 3C_3^{(1,2)} &= \{ba^2, baa', ba'^2\}, \\ 3C_3^{(2,0)} &= \{b^2, b^2aa'^2, b^2a^2a'\}, \\ 3C_3^{(2,1)} &= \{b^2a, b^2a', b^2a^2a'^2\}, \\ 3C_3^{(2,2)} &= \{b^2a^2, b^2aa', b^2a'^2\}. \end{aligned} \quad (\text{A2})$$

The $\Delta(27)$ has nine one dimensional representations, which we denote as $\mathbf{1}_{k,r}$ ($k, r = 0, 1, 2$), and two three dimensional irreducible representations $\mathbf{3}$ and $\bar{\mathbf{3}}$. The explicit form of the group generators in each irreducible representation

	$\chi_{1_{0,0}}$	$\chi_{1_{0,1}}$	$\chi_{1_{0,2}}$	$\chi_{1_{1,0}}$	$\chi_{1_{1,1}}$	$\chi_{1_{1,2}}$	$\chi_{1_{2,0}}$	$\chi_{1_{2,1}}$	$\chi_{1_{2,2}}$	$\chi_{\mathbf{3}}$	$\chi_{\overline{\mathbf{3}}}$
$1C_1$	1	1	1	1	1	1	1	1	1	3	3
$1C_1^{(1)}$	1	1	1	1	1	1	1	1	1	$3\omega^2$	3ω
$1C_1^{(2)}$	1	1	1	1	1	1	1	1	1	3ω	$3\omega^2$
$3C_3^{(0,1)}$	1	ω	ω^2	1	ω	ω^2	1	ω	ω^2	0	0
$3C_3^{(0,2)}$	1	ω^2	ω	1	ω^2	ω	1	ω^2	ω	0	0
$3C_3^{(1,0)}$	1	1	1	ω	ω	ω	ω^2	ω^2	ω^2	0	0
$3C_3^{(1,1)}$	1	ω	ω^2	ω	ω^2	1	ω^2	1	ω	0	0
$3C_3^{(1,2)}$	1	ω^2	ω	ω	1	ω^2	ω^2	ω	1	0	0
$3C_3^{(2,0)}$	1	1	1	ω^2	ω^2	ω^2	ω	ω	ω	0	0
$3C_3^{(2,1)}$	1	ω	ω^2	ω^2	1	ω	ω	ω^2	1	0	0
$3C_3^{(2,2)}$	1	ω^2	ω	ω^2	ω	1	ω	1	ω^2	0	0

TABLE VI: Character table of $\Delta(27)$.

is

$$\begin{aligned}
\mathbf{1}_{k,r} : & \quad a = \omega^r, & a' = \omega^r, & b = \omega^k, \\
\mathbf{3} : & \quad a = \begin{pmatrix} \omega & 0 & 0 \\ 0 & 1 & 0 \\ 0 & 0 & \omega^2 \end{pmatrix}, & a' = \begin{pmatrix} \omega^2 & 0 & 0 \\ 0 & \omega & 0 \\ 0 & 0 & 1 \end{pmatrix}, & b = \begin{pmatrix} 0 & 1 & 0 \\ 0 & 0 & 1 \\ 1 & 0 & 0 \end{pmatrix}, \\
\overline{\mathbf{3}} : & \quad a = \begin{pmatrix} \omega^2 & 0 & 0 \\ 0 & 1 & 0 \\ 0 & 0 & \omega \end{pmatrix}, & a' = \begin{pmatrix} \omega & 0 & 0 \\ 0 & \omega^2 & 0 \\ 0 & 0 & 1 \end{pmatrix}, & b = \begin{pmatrix} 0 & 1 & 0 \\ 0 & 0 & 1 \\ 1 & 0 & 0 \end{pmatrix},
\end{aligned} \tag{A3}$$

where $\omega = e^{2\pi i/3}$ is the cube root of unity. Notice that $\mathbf{3}$ and $\overline{\mathbf{3}}$ are complex representations dual to each other. From the character table of the group, shown in Table VI, we can straightforwardly obtain the Kronecker products between the various representations

$$\begin{aligned}
\mathbf{1}_{k,r} \otimes \mathbf{1}_{k',r'} &= \mathbf{1}_{[k+k'],[r+r']}, & \mathbf{3} \otimes \mathbf{1}_{k,r} &= \mathbf{3}, & \overline{\mathbf{3}} \otimes \mathbf{1}_{k,r} &= \overline{\mathbf{3}}, \\
\mathbf{3} \otimes \overline{\mathbf{3}} &= \sum_{k,r=0}^2 \mathbf{1}_{k,r}, & \mathbf{3} \otimes \mathbf{3} &= \overline{\mathbf{3}} \oplus \overline{\mathbf{3}} \oplus \overline{\mathbf{3}}, & \overline{\mathbf{3}} \otimes \overline{\mathbf{3}} &= \mathbf{3} \oplus \mathbf{3} \oplus \mathbf{3},
\end{aligned} \tag{A4}$$

where $[n]$ stands for $n \bmod 3$, whenever n is an integer. Starting from the representation matrices of the generators in different irreducible representations, we can calculate the Clebsch-Gordan (CG) coefficients for the Kronecker products listed above. All CG coefficients are presented in the form $\alpha \otimes \beta$, where α_i stands for the elements of the first representation and β_j those of the second one. In the following, we adopt the convention $\alpha_{[3]} = \alpha_0 \equiv \alpha_3$.

- $\mathbf{1}_{k,r} \otimes \mathbf{1}_{k',r'} = \mathbf{1}_{[k+k'],[r+r']}$

$$\left(\alpha_1 \right)_{\mathbf{1}_{k,r}} \otimes \left(\beta_1 \right)_{\mathbf{1}_{k',r'}} = \left(\alpha_1 \beta_1 \right)_{\mathbf{1}_{[k+k'],[r+r']}}.$$

- $\mathbf{3} \otimes \mathbf{1}_{k,r} = \mathbf{3}$

$$\begin{pmatrix} \alpha_1 \\ \alpha_2 \\ \alpha_3 \end{pmatrix}_{\mathbf{3}} \otimes \left(\beta_1 \right)_{\mathbf{1}_{k,r}} = \begin{pmatrix} \alpha_{[1+r]}\beta_1 \\ \omega^k \alpha_{[2+r]}\beta_1 \\ \omega^{2k} \alpha_{[3+r]}\beta_1 \end{pmatrix}_{\mathbf{3}}.$$

- $\bar{\mathbf{3}} \otimes \mathbf{1}_{k,r} = \bar{\mathbf{3}}$

$$\begin{pmatrix} \alpha_1 \\ \alpha_2 \\ \alpha_3 \end{pmatrix}_{\bar{\mathbf{3}}} \otimes \begin{pmatrix} \beta_1 \end{pmatrix}_{\mathbf{1}_{k,r}} = \begin{pmatrix} \alpha_{[1-r]}\beta_1 \\ \omega^k \alpha_{[2-r]}\beta_1 \\ \omega^{2k} \alpha_{[3-r]}\beta_1 \end{pmatrix}_{\bar{\mathbf{3}}}.$$

- $\mathbf{3} \otimes \bar{\mathbf{3}} = \sum_{k,r=0}^2 \mathbf{1}_{k,r}$

$$\begin{aligned} & \begin{pmatrix} \alpha_1 \\ \alpha_2 \\ \alpha_3 \end{pmatrix}_{\mathbf{3}} \otimes \begin{pmatrix} \beta_1 \\ \beta_2 \\ \beta_3 \end{pmatrix}_{\bar{\mathbf{3}}} \\ &= (\alpha_1\beta_1 + \alpha_2\beta_2 + \alpha_3\beta_3)_{\mathbf{1}_{0,0}} \oplus (\alpha_1\beta_1 + \omega^2\alpha_2\beta_2 + \omega\alpha_3\beta_3)_{\mathbf{1}_{1,0}} \oplus (\alpha_1\beta_1 + \omega\alpha_2\beta_2 + \omega^2\alpha_3\beta_3)_{\mathbf{1}_{2,0}} \\ & \oplus (\alpha_3\beta_1 + \alpha_1\beta_2 + \alpha_2\beta_3)_{\mathbf{1}_{0,1}} \oplus (\alpha_3\beta_1 + \omega^2\alpha_1\beta_2 + \omega\alpha_2\beta_3)_{\mathbf{1}_{1,1}} \oplus (\alpha_3\beta_1 + \omega\alpha_1\beta_2 + \omega^2\alpha_2\beta_3)_{\mathbf{1}_{2,1}} \\ & \oplus (\alpha_2\beta_1 + \alpha_3\beta_2 + \alpha_1\beta_3)_{\mathbf{1}_{0,2}} \oplus (\alpha_2\beta_1 + \omega^2\alpha_3\beta_2 + \omega\alpha_1\beta_3)_{\mathbf{1}_{1,2}} \oplus (\alpha_2\beta_1 + \omega\alpha_3\beta_2 + \omega^2\alpha_1\beta_3)_{\mathbf{1}_{2,2}}. \end{aligned}$$

- $\mathbf{3} \otimes \mathbf{3} = \bar{\mathbf{3}}_{S_1} \oplus \bar{\mathbf{3}}_{S_2} \oplus \bar{\mathbf{3}}_A$

$$\begin{pmatrix} \alpha_1 \\ \alpha_2 \\ \alpha_3 \end{pmatrix}_{\mathbf{3}} \otimes \begin{pmatrix} \beta_1 \\ \beta_2 \\ \beta_3 \end{pmatrix}_{\mathbf{3}} = \begin{pmatrix} \alpha_1\beta_1 \\ \alpha_2\beta_2 \\ \alpha_3\beta_3 \end{pmatrix}_{\bar{\mathbf{3}}_{S_1}} \oplus \frac{1}{2} \begin{pmatrix} \alpha_2\beta_3 + \alpha_3\beta_2 \\ \alpha_3\beta_1 + \alpha_1\beta_3 \\ \alpha_1\beta_2 + \alpha_2\beta_1 \end{pmatrix}_{\bar{\mathbf{3}}_{S_2}} \oplus \frac{1}{2} \begin{pmatrix} \alpha_2\beta_3 - \alpha_3\beta_2 \\ \alpha_3\beta_1 - \alpha_1\beta_3 \\ \alpha_1\beta_2 - \alpha_2\beta_1 \end{pmatrix}_{\bar{\mathbf{3}}_A}, \quad (\text{A5})$$

where the subscripts ‘‘S’’ and ‘‘A’’ denote symmetric and anti-symmetric combinations respectively.

- $\bar{\mathbf{3}} \otimes \bar{\mathbf{3}} = \mathbf{3}_{S_1} \oplus \mathbf{3}_{S_2} \oplus \mathbf{3}_A$

$$\begin{pmatrix} \alpha_1 \\ \alpha_2 \\ \alpha_3 \end{pmatrix}_{\bar{\mathbf{3}}} \otimes \begin{pmatrix} \beta_1 \\ \beta_2 \\ \beta_3 \end{pmatrix}_{\bar{\mathbf{3}}} = \begin{pmatrix} \alpha_1\beta_1 \\ \alpha_2\beta_2 \\ \alpha_3\beta_3 \end{pmatrix}_{\mathbf{3}_{S_1}} \oplus \frac{1}{2} \begin{pmatrix} \alpha_2\beta_3 + \alpha_3\beta_2 \\ \alpha_3\beta_1 + \alpha_1\beta_3 \\ \alpha_1\beta_2 + \alpha_2\beta_1 \end{pmatrix}_{\mathbf{3}_{S_2}} \oplus \frac{1}{2} \begin{pmatrix} \alpha_2\beta_3 - \alpha_3\beta_2 \\ \alpha_3\beta_1 - \alpha_1\beta_3 \\ \alpha_1\beta_2 - \alpha_2\beta_1 \end{pmatrix}_{\mathbf{3}_A}. \quad (\text{A6})$$

Appendix B: Vacuum Alignment

In this Appendix, we shall investigate the problem of achieving the vacuum configuration in Eq. (10) and Eq. (11). For self-consistency, all flavon fields φ , ξ , σ_1 and σ_2 are treated as complex, given the form of the $\Delta(27)$ representation matrices, and the fact that the Z_4 charge of σ_2 is purely imaginary. Since the flavons φ and ξ , σ_1 , σ_2 are assumed to be localized at $y = 0$ and $y = L$ respectively, the vacuum alignment problem is greatly simplified. At the UV brane $y = 0$, the flavon φ transforms in the manner listed in Table I. The scalar potential invariant under the flavor symmetry $\Delta(27) \otimes Z_4 \otimes Z'_4$ can be written as:

$$\begin{aligned} V_{\text{UV}} &= M_\varphi^2 (\varphi\varphi^*)_{\mathbf{1}_{0,0}} + f_1 \left[(\varphi\varphi)_{\bar{\mathbf{3}}_{S_1}} (\varphi^*\varphi^*)_{\mathbf{3}_{S_1}} \right]_{\mathbf{1}_{0,0}} + f_2 \left[(\varphi\varphi)_{\bar{\mathbf{3}}_{S_2}} (\varphi^*\varphi^*)_{\mathbf{3}_{S_2}} \right]_{\mathbf{1}_{0,0}} \\ & \quad + f_3 \left[(\varphi\varphi)_{\bar{\mathbf{3}}_{S_1}} (\varphi^*\varphi^*)_{\mathbf{3}_{S_2}} \right]_{\mathbf{1}_{0,0}} + f_3^* \left[(\varphi\varphi)_{\bar{\mathbf{3}}_{S_2}} (\varphi^*\varphi^*)_{\mathbf{3}_{S_1}} \right]_{\mathbf{1}_{0,0}}, \end{aligned} \quad (\text{B1})$$

with real couplings M_φ^2 , f_1 and f_2 . Note that $\varphi = (\varphi_1, \varphi_2, \varphi_3)$ is a $\Delta(27)$ triplet $\mathbf{3}$, and its complex conjugate $\varphi^* = (\varphi_1^*, \varphi_2^*, \varphi_3^*)$ transforms consequently as $\bar{\mathbf{3}}$. Focusing on the field configuration

$$\langle \varphi \rangle = (1, 1, 1)v_\varphi, \quad (\text{B2})$$

the minimum conditions for the UV potential read

$$\frac{\partial V_{\text{UV}}}{\partial \varphi_1^*} = \frac{\partial V_{\text{UV}}}{\partial \varphi_2^*} = \frac{\partial V_{\text{UV}}}{\partial \varphi_3^*} = v_\varphi \left[M_\varphi^2 + 2(f_1 + f_2 + f_3 + f_3^*) |v_\varphi|^2 \right] = 0, \quad (\text{B3})$$

leading to a non zero solution

$$|v_\varphi|^2 = -\frac{M_\varphi^2}{2(f_1 + f_2 + f_3 + f_3^*)}, \quad (\text{B4})$$

that holds in a finite portion of parameter space with $f_1 + f_2 + f_3 + f_3^* < 0$.

Similarly, at the IR brane $y = L$, the most general renormalizable scalar potential V_{IR} involving the flavon fields ξ , σ_1 , σ_2 is

$$\begin{aligned} V_{\text{IR}} = & M_\xi^2 (\xi \xi^*)_{\mathbf{1}_{0,0}} + M_{\sigma_1}^2 (\sigma_1 \sigma_1^*)_{\mathbf{1}_{0,0}} + M_{\sigma_2}^2 (\sigma_2 \sigma_2^*)_{\mathbf{1}_{0,0}} + g_1 \left[(\xi \xi)_{\overline{\mathbf{3}}_{S_1}} (\xi^* \xi^*)_{\mathbf{3}_{S_1}} \right]_{\mathbf{1}_{0,0}} \\ & + g_2 \left[(\xi \xi)_{\overline{\mathbf{3}}_{S_2}} (\xi^* \xi^*)_{\mathbf{3}_{S_2}} \right]_{\mathbf{1}_{0,0}} + g_3 \left[(\xi \xi)_{\overline{\mathbf{3}}_{S_1}} (\xi^* \xi^*)_{\mathbf{3}_{S_2}} \right]_{\mathbf{1}_{0,0}} + g_3^* \left[(\xi \xi)_{\overline{\mathbf{3}}_{S_2}} (\xi^* \xi^*)_{\mathbf{3}_{S_1}} \right]_{\mathbf{1}_{0,0}} \\ & + g_4 \sigma_1^2 \sigma_1^{*2} + g_5 \sigma_2^2 \sigma_2^{*2} + g_6 |\sigma_1|^2 |\sigma_2|^2 + g_7 (\xi \xi^*)_{\mathbf{1}_{0,0}} |\sigma_1|^2 + g_8 (\xi \xi^*)_{\mathbf{1}_{0,0}} |\sigma_2|^2 \\ & + g_9 (\xi \xi^*)_{\mathbf{1}_{0,1}} \sigma_1^2 + g_9^* (\xi \xi^*)_{\mathbf{1}_{0,2}} \sigma_1^{*2}, \end{aligned} \quad (\text{B5})$$

where all couplings, excluding g_3 and g_9 , are real. For this potential, the Case I alignment

$$\langle \xi \rangle = (0, v_\xi, 0), \quad \langle \sigma_1 \rangle = v_{\sigma_1}, \quad \langle \sigma_2 \rangle = v_{\sigma_2}, \quad (\text{B6})$$

determines the minimization conditions

$$\begin{aligned} \frac{\partial V_{\text{IR}}}{\partial \xi_1^*} &= g_9^* v_\xi v_{\sigma_1}^{*2} = 0, \\ \frac{\partial V_{\text{IR}}}{\partial \xi_2^*} &= v_\xi \left(M_\xi^2 + 2g_1 |v_\xi|^2 + g_7 |v_{\sigma_1}|^2 + g_8 |v_{\sigma_2}|^2 \right) = 0, \\ \frac{\partial V_{\text{IR}}}{\partial \xi_3^*} &= g_9 v_\xi v_{\sigma_1}^2 = 0, \\ \frac{\partial V_{\text{IR}}}{\partial \sigma_1^*} &= v_{\sigma_1} \left(M_{\sigma_1}^2 + 2g_4 |v_{\sigma_1}|^2 + g_7 |v_\xi|^2 + g_6 |v_{\sigma_2}|^2 \right) = 0, \\ \frac{\partial V_{\text{IR}}}{\partial \sigma_2^*} &= v_{\sigma_2} \left(M_{\sigma_2}^2 + 2g_5 |v_{\sigma_2}|^2 + g_8 |v_\xi|^2 + g_6 |v_{\sigma_1}|^2 \right) = 0. \end{aligned} \quad (\text{B7})$$

From the above equations, it is clear that non-trivial solutions in this sector are only achievable by fine tuning the g_9 parameter to satisfy $g_9 = 0$. This choice can be enforced by an additional dynamical mechanism capable of switching off the $(\xi \xi^*)_{\mathbf{1}_{0,1}} \sigma_1^2$ and $(\xi \xi^*)_{\mathbf{1}_{0,2}} \sigma_1^{*2}$ terms in the potential. Such scenario could be naturally realized in a supersymmetric extension [20, 45]. As this possibility lies beyond the scope of the present work, we simply impose the condition $g_9 = 0$ in the general potential. Then, the obtained solutions are given by

$$\begin{aligned} |v_\xi|^2 &= \frac{(g_6^2 - 4g_4g_5)M_\xi^2 + (2g_5g_7 - g_6g_8)M_{\sigma_1}^2 + (2g_4g_8 - g_6g_7)M_{\sigma_2}^2}{2(4g_1g_4g_5 + g_6g_7g_8 - g_1g_6^2 - g_4g_8^2 - g_5g_7^2)}, \\ |v_{\sigma_1}|^2 &= \frac{(2g_5g_7 - g_6g_8)M_\xi^2 + (g_8^2 - 4g_1g_5)M_{\sigma_1}^2 + (2g_1g_6 - g_7g_8)M_{\sigma_2}^2}{2(4g_1g_4g_5 + g_6g_7g_8 - g_1g_6^2 - g_4g_8^2 - g_5g_7^2)}, \\ |v_{\sigma_2}|^2 &= \frac{(2g_4g_8 - g_6g_7)M_\xi^2 + (2g_1g_6 - g_7g_8)M_{\sigma_1}^2 + (g_7^2 - 4g_1g_4)M_{\sigma_2}^2}{2(4g_1g_4g_5 + g_6g_7g_8 - g_1g_6^2 - g_4g_8^2 - g_5g_7^2)}. \end{aligned} \quad (\text{B8})$$

The right-handed side of these expressions can be positive in a finite region of parameter space. Analogously, for the Case II vacuum configuration

$$\langle \xi \rangle = (1, \omega, 1)v_\xi, \quad \langle \sigma_1 \rangle = v_{\sigma_1}, \quad \langle \sigma_2 \rangle = v_{\sigma_2}, \quad (\text{B9})$$

the minimization conditions are

$$\begin{aligned}
\frac{\partial V_{\text{IR}}}{\partial \xi_1^*} &= v_\xi \left[M_\xi^2 + 2(g_1 + g_2 + \omega^2 g_3 + \omega g_3^*) |v_\xi|^2 + g_7 |v_{\sigma_1}|^2 + g_8 |v_{\sigma_2}|^2 + g_9 v_{\sigma_1}^2 + \omega g_9^* v_{\sigma_1}^{*2} \right] = 0, \\
\frac{\partial V_{\text{IR}}}{\partial \xi_2^*} &= \omega v_\xi \left[M_\xi^2 + 2(g_1 + g_2 + \omega^2 g_3 + \omega g_3^*) |v_\xi|^2 + g_7 |v_{\sigma_1}|^2 + g_8 |v_{\sigma_2}|^2 + \omega^2 g_9 v_{\sigma_1}^2 + \omega^2 g_9^* v_{\sigma_1}^{*2} \right] = 0, \\
\frac{\partial V_{\text{IR}}}{\partial \xi_3^*} &= v_\xi \left[M_\xi^2 + 2(g_1 + g_2 + \omega^2 g_3 + \omega g_3^*) |v_\xi|^2 + g_7 |v_{\sigma_1}|^2 + g_8 |v_{\sigma_2}|^2 + \omega g_9 v_{\sigma_1}^2 + g_9^* v_{\sigma_1}^{*2} \right] = 0, \\
\frac{\partial V_{\text{IR}}}{\partial \sigma_1^*} &= v_{\sigma_1} \left[M_{\sigma_1}^2 + 2g_4 |v_{\sigma_1}|^2 + g_6 |v_{\sigma_2}|^2 + 3g_7 |v_\xi|^2 \right] = 0, \\
\frac{\partial V_{\text{IR}}}{\partial \sigma_2^*} &= v_{\sigma_2} \left[M_{\sigma_2}^2 + 2g_5 |v_{\sigma_2}|^2 + g_6 |v_{\sigma_1}|^2 + 3g_8 |v_\xi|^2 \right] = 0.
\end{aligned} \tag{B10}$$

Again, these equations are incompatible unless $g_9 = 0$. Once the coupling g_9 is enforced to vanish, we are left with three independent linear equations for the three unknown variables v_ξ , v_{σ_1} and v_{σ_2} . The solutions can be easily found as

$$\begin{aligned}
|v_\xi|^2 &= \frac{(4g_4g_5 - g_6^2)M_\xi^2 + (g_6g_8 - 2g_5g_7)M_{\sigma_1}^2 + (g_6g_7 - 2g_4g_8)M_{\sigma_2}^2}{2\tilde{g}(g_6^2 - 4g_4g_5) + 6(g_4g_8^2 + g_5g_7^2 - g_6g_7g_8)}, \\
|v_{\sigma_1}|^2 &= \frac{(3g_6g_8 - 6g_5g_7)M_\xi^2 + (4\tilde{g}g_5 - 3g_8^2)M_{\sigma_1}^2 + (3g_7g_8 - 2\tilde{g}g_6)M_{\sigma_2}^2}{2\tilde{g}(g_6^2 - 4g_4g_5) + 6(g_4g_8^2 + g_5g_7^2 - g_6g_7g_8)}, \\
|v_{\sigma_2}|^2 &= \frac{(3g_6g_7 - 6g_4g_8)M_\xi^2 + (3g_7g_8 - 2\tilde{g}g_6)M_{\sigma_1}^2 + (4\tilde{g}g_4 - 3g_7^2)M_{\sigma_2}^2}{2\tilde{g}(g_6^2 - 4g_4g_5) + 6(g_4g_8^2 + g_5g_7^2 - g_6g_7g_8)}.
\end{aligned} \tag{B11}$$

where we have defined $\tilde{g} \equiv g_1 + g_2 + \omega^2 g_3 + \omega g_3^*$. Therefore, both $\langle \xi \rangle = (0, v_\xi, 0)$ and $\langle \xi \rangle = (1, \omega, 1)v_\xi$ alignments can describe the local minimum of V_{IR} , depending on the the parameter values. In the case of $g_1 \ll \tilde{g}$, the VEV $\langle \xi \rangle = (0, v_\xi, 0)$ is preferred over $\langle \xi \rangle = (1, \omega, 1)v_\xi$, while V_{IR} is minimized by $\langle \xi \rangle = (1, \omega, 1)v_\xi$ for $g_1 \gg \tilde{g}$.

-
- [1] K. A. Olive *et al.* [Particle Data Group Collaboration], *Chin. Phys. C* **38** (2014) 090001.
[2] K. S. Babu, E. Ma and J. W. F. Valle, *Phys. Lett. B* **552** (2003) 207 [hep-ph/0206292].
[3] S. Morisi and J. W. F. Valle, *Fortsch. Phys.* **61** (2013) 466 [arXiv:1206.6678 [hep-ph]].
[4] G. Altarelli, F. Feruglio, L. Merlo and E. Stamou, *JHEP* **1208** (2012) 021 [arXiv:1205.4670 [hep-ph]].
[5] R. M. Fonseca and W. Grimus, arXiv:1410.4133 [hep-ph].
[6] G. Altarelli and F. Feruglio, *Rev. Mod. Phys.* **82** (2010) 2701 [arXiv:1002.0211 [hep-ph]].
[7] H. Ishimori, T. Kobayashi, H. Ohki, Y. Shimizu, H. Okada and M. Tanimoto, *Prog. Theor. Phys. Suppl.* **183** (2010) 1 [arXiv:1003.3552 [hep-th]].
[8] S. F. King and C. Luhn, *Rept. Prog. Phys.* **76** (2013) 056201 [arXiv:1301.1340 [hep-ph]].
[9] S. F. King, A. Merle, S. Morisi, Y. Shimizu and M. Tanimoto, *New J. Phys.* **16** (2014) 045018 [arXiv:1402.4271 [hep-ph]].
[10] P. F. Harrison, D. H. Perkins and W. G. Scott, *Phys. Lett. B* **530** (2002) 167 [hep-ph/0202074].
[11] F. P. An *et al.* [Daya Bay Collaboration], *Phys. Rev. Lett.* **108** (2012) 171803 [arXiv:1203.1669 [hep-ex]].
[12] K. Abe *et al.* [T2K Collaboration], *Phys. Rev. Lett.* **107** (2011) 041801 [arXiv:1106.2822 [hep-ex]].
[13] P. Adamson *et al.* [MINOS Collaboration], *Phys. Rev. Lett.* **110** (2013) 25, 251801 [arXiv:1304.6335 [hep-ex]].
[14] J. K. Ahn *et al.* [RENO Collaboration], *Phys. Rev. Lett.* **108** (2012) 191802 [arXiv:1204.0626 [hep-ex]].
[15] S. Morisi, D. V. Forero, J. C. Romo and J. W. F. Valle, *Phys. Rev. D* **88** (2013) 1, 016003 [arXiv:1305.6774 [hep-ph]].
[16] S. M. Boucenna, S. Morisi, M. Tortola and J. W. F. Valle, *Phys. Rev. D* **86** (2012) 051301 [arXiv:1206.2555 [hep-ph]].
[17] G. J. Ding, S. Morisi and J. W. F. Valle, *Phys. Rev. D* **87** (2013) 5, 053013 [arXiv:1211.6506 [hep-ph]].
[18] S. Roy and N. N. Singh, *Indian J. Phys.* **88** (2014) 5, 513 [arXiv:1211.7207 [hep-ph]].
[19] L. Randall and R. Sundrum, *Phys. Rev. Lett.* **83** (1999) 3370 [hep-ph/9905221].
[20] G. Altarelli and F. Feruglio, *Nucl. Phys. B* **720** (2005) 64 [hep-ph/0504165].
[21] G. Altarelli, F. Feruglio and C. Hagedorn, *JHEP* **0803** (2008) 052 [arXiv:0802.0090 [hep-ph]].

- [22] T. J. Burrows and S. F. King, Nucl. Phys. B **835** (2010) 174 [arXiv:0909.1433 [hep-ph]].
- [23] C. Csaki, C. Delaunay, C. Grojean and Y. Grossman, JHEP **0810** (2008) 055 [arXiv:0806.0356 [hep-ph]].
- [24] M. C. Chen, K. T. Mahanthappa and F. Yu, Phys. Rev. D **81** (2010) 036004 [arXiv:0907.3963 [hep-ph]].
- [25] A. Kadosh and E. Pallante, JHEP **1008** (2010) 115 [arXiv:1004.0321 [hep-ph]].
- [26] A. Kadosh and E. Pallante, JHEP **1106** (2011) 121 [arXiv:1101.5420 [hep-ph]].
- [27] A. Kadosh, JHEP **1306** (2013) 114 [arXiv:1303.2645 [hep-ph]].
- [28] F. del Aguila, A. Carmona and J. Santiago, JHEP **1008** (2010) 127 [arXiv:1001.5151 [hep-ph]].
- [29] C. Hagedorn and M. Serone, JHEP **1202** (2012) 077 [arXiv:1110.4612 [hep-ph]].
- [30] C. Hagedorn and M. Serone, JHEP **1110** (2011) 083 [arXiv:1106.4021 [hep-ph]].
- [31] D. V. Forero, M. Tortola and J. W. F. Valle, Phys. Rev. D **90** (2014) 9, 093006 [arXiv:1405.7540 [hep-ph]].
- [32] G. J. Ding and Y. L. Zhou, Nucl. Phys. B **876** (2013) 418 [arXiv:1304.2645 [hep-ph]].
- [33] K. Agashe, A. Delgado, M. J. May and R. Sundrum, JHEP **0308** (2003) 050 [hep-ph/0308036].
- [34] K. Agashe, R. Contino, L. Da Rold and A. Pomarol, Phys. Lett. B **641** (2006) 62 [hep-ph/0605341].
- [35] G. Cacciapaglia, C. Csaki, G. Marandella and J. Terning, JHEP **0702** (2007) 036 [hep-ph/0611358].
- [36] T. Gherghetta and A. Pomarol, Nucl. Phys. B **586** (2000) 141 [hep-ph/0003129].
- [37] Y. Grossman and M. Neubert, Phys. Lett. B **474** (2000) 361 [hep-ph/9912408].
- [38] S. J. Huber and Q. Shafi, Phys. Lett. B **512** (2001) 365 [hep-ph/0104293].
- [39] I. de Medeiros Varzielas, S. F. King and G. G. Ross, Phys. Lett. B **648** (2007) 201 [hep-ph/0607045].
- [40] E. Ma, Mod. Phys. Lett. A **21** (2006) 1917 [hep-ph/0607056].
- [41] A. Aranda, C. Bonilla, S. Morisi, E. Peinado and J. W. F. Valle, Phys. Rev. D **89** (2014) 3, 033001 [arXiv:1307.3553 [hep-ph]].
- [42] G. C. Branco, J. M. Gerard and W. Grimus, Phys. Lett. B **136** (1984) 383.
- [43] G. Bhattacharyya, I. de Medeiros Varzielas and P. Leser, Phys. Rev. Lett. **109** (2012) 241603 [arXiv:1210.0545 [hep-ph]].
- [44] C. Jarlskog, Phys. Rev. Lett. **55** (1985) 1039.
- [45] G. Altarelli and F. Feruglio, Nucl. Phys. B **741** (2006) 215 [hep-ph/0512103].